https://doi.org/10.5194/egusphere-2026-2895
Preprint. Discussion started: 18 June 2026

Assessing summertime hydrological cycle acceleration through drought indices.

Matthew W. Sabin[1], Nels Bjarke[1,2,3], Ben Livneh[1,2,3]

[1] Department of Civil, Environmental, and Architectural Engineering, University of Colorado, Boulder, 80309, United States
[2] Cooperative Institute for Research in Environmental Sciences, University of Colorado, Boulder, 80309, United States
[3] Western Water Assessment, University of Colorado, Boulder, 80309, United States

Correspondence to: Matthew W. Sabin (matthew.sabin@colorado.edu)

Abstract. The rate (or velocity) of the hydrological cycle affects water availability for agriculture, energy production, and planning for droughts or floods. Therefore, acceleration in the velocity of the hydrological cycle is likely to impact multiple hydrological domains and management practices. Previous work has primarily studied hydrological cycle velocity and acceleration through the lens of flux magnitudes and their change. Motivated to expand this definition to characterize temporal coupling between stages in the hydrological cycle, we introduce a novel definition of hydrological cycle velocity and acceleration derived from the concept of drought propagation. We define the hydrological cycle velocity as the response time between the 1-month Standardized Precipitation Index (SPI) and the 1-month Standardized Soil Moisture Index (SSI) and define acceleration as the change in response time between an early time period and a late period. Using gridded reanalysis data over the conterminous United States (CONUS) from 1951-2020, we analyzed the summer period (June, July, August) to minimize the lagging-effects of cold-season processes. Response times exceeded 100 days in southwestern CONUS (indicating a slower hydrological cycle velocity), but were substantially shorter elsewhere, 10-20 days, indicating a faster hydrological cycle velocity. A Random Forest variable importance analysis revealed strong negative associations of response time and mean annual flux magnitudes, with higher precipitation and evaporation associated with shorter response times. Regarding potential acceleration between an earlier (1951-1985) and later (1986-2020) period, 48.47 % of reanalysis grid cells experienced a deceleration (lengthening of response time) of their local summer hydrological cycle, while 39.32 % of grid cells experienced an acceleration (shortening of response time). However, a false detection rate correction found a lack of robust field significance (α_{FDR}=0.05), a finding reinforced by a regional decadal trend analysis. By framing hydrological cycle acceleration in terms of propagation of meteorological anomalies to land surface anomalies, we expand the conceptual basis for diagnosing changes in the hydrological cycle.

1 Introduction

Hydrological cycle change has been a prominent feature of the last century. Altered precipitation intensity (Contractor et al., 2021; Giorgi et al., 2011), drought characteristics (Dai, 2013; Williams et al., 2020; Yuan et al., 2023), runoff trends (Dai, 2016; Xiao et al., 2018), and atmospheric demand (Vicente-Serrano et al., 2022) are among the notable

https://doi.org/10.5194/egusphere-2026-2895
Preprint. Discussion started: 18 June 2026

observed changes. Changes in the rate (velocity) of hydrological processes can have widespread impacts on water availability and water resource planning (Musselman et al., 2017; Vicente-Serrano et al., 2014; Wang et al., 2023), motivating growing interest in whether the hydrological cycle is accelerating. Approaches have largely fallen into three categories: quantifying changes in the magnitude of a single hydrological flux or variable (Ohmura and Wild, 2002; Yeh and Wu, 2018), analyzing changes in the magnitude of a combination of hydrological fluxes or variables (Feng et al., 2017; Huntington et al., 2018; Vargas Godoy and Markonis, 2023), or calculating changes to the residence time of water in a hydrological storage component (Held and Soden, 2006; Kao et al., 2018; Li et al., 2011; Wang et al., 2023). However, a gap remains in understanding whether the temporal coupling between stages in the hydrological cycle is changing. To address this gap, we expand on the lag characteristic of drought propagation (Van Loon et al., 2012) to introduce a novel metric of hydrological cycle acceleration. Basing our approach on the physical assumption that hydrological anomalies in the atmosphere typically precede anomalies on the land surface, we define hydrological cycle acceleration as a decrease in the time it takes meteorological anomalies to propagate into soil moisture anomalies. Using drought indices to quantify these anomalies, our approach seeks to provide a meaningful contribution to the question of hydrological cycle acceleration in terms of indices already familiar to land managers (Hawkes et al., 2018; Svoboda et al., 2002).

1.1 Existing definitions of hydrological cycle acceleration

Many terms exist to describe the types of hydrological change we are interested in, with intensification and acceleration among the most common. Although sometimes used interchangeably by researchers, we distinguish them here for clarity. We define *intensification* as changes in the magnitude of hydrological fluxes (Huntington et al., 2018), and *acceleration* as changes in the degree of temporal coupling between stages of the hydrological cycle, quantified through metrics such as the residence time of water in the soil (Gimeno et al., 2021; Kao et al., 2018; Li et al., 2011; Wang et al., 2023). Because metrics of intensification and acceleration do not always change in tandem (discussed in Sect. 1.1.3), distinguishing them is important to gain a clearer understanding of hydrological cycle change. This study focuses on *acceleration*. We use the term velocity to describe a static, intra-period temporal metric, and acceleration to describe the inter-period change in a temporal metric.

1.1.1 Changes in a single flux

The simplest way to quantify hydrological cycle change is by examining trends in individual hydrological fluxes. This approach is appealing due to its straightforward interpretability and the reduced uncertainty provided by the relatively long, reliable observational records available for certain fluxes, i.e., precipitation (P) and runoff. However, changes in a particular term of the water balance do not necessarily reflect changes in the entire hydrological cycle. For example, runoff in the Upper Colorado River Basin declined by 16.5% from 1916-2014 despite a slight increase in precipitation (Xiao et al., 2018).

Theoretically, increases in global temperature are expected to enhance both P and evapotranspiration (E) through Clausius-Clapeyron scaling and changes in the tropospheric energy balance (Allen and Ingram, 2002; Held and Soden, 2006). For precipitation, this expectation is generally supported by model- and observation-based studies (Hobeichi

https://doi.org/10.5194/egusphere-2026-2895
Preprint. Discussion started: 18 June 2026

et al., 2022; Liu and Allan, 2013; Trenberth, 2011), although Adler et al. (2017) found no global trend during the satellite era. Regional variability is substantial in these studies. Evidence for evapotranspiration trends is more uncertain due to limited direct observations, leading to greater regional variability and inter-study disagreements in both the magnitude and direction of change (Hobeichi et al., 2022; Jung et al., 2010; Zhang et al., 2016). Although single-flux analyses are practical and intuitive, they provide only a partial view of hydrological cycle change and, under our definitions, primarily represent measures of intensification rather than acceleration.

1.1.2 Change in water cycle intensity

A more comprehensive approach to characterizing hydrological change combines multiple fluxes, most commonly P and E. Including additional terms provides a more complete accounting of hydrological change but also introduces more uncertainty, particularly given the poor observational record of E. Huntington et al. (2018) coined the term Water Cycle Intensity (WCI), defined as P+E, to investigate hydrological cycle *intensification*, finding a generally positive (although often statistically insignificant at the regional level) trend across the conterminous United States (CONUS) from 1945-2014. They posit that when paired with a water balance equation, understanding changes in WCI and its components over land enables insights into changing soil moisture storage and runoff. Other studies have used P+E as an indicator of hydrological cycle *acceleration*, characterizing increases in global P+E across four reanalysis datasets as evidence of hydrological cycle acceleration (Vargas Godoy and Markonis, 2023). Feng et al. (2017) analyzed the spatial trends in P+E over land, finding that approximately 32% of global land surfaces experienced an accelerating hydrological cycle from 1982-2011, while 10% of the global land surface experienced a decelerating hydrological cycle. Differences between acceleration and intensification are not delineated in those studies. Changes in P+E provide useful information about hydrological change, but because it represents the total flux in and out of the land surface, it is best categorized as intensification rather than acceleration under our definitions.

An alternative metric, HY-INT (Giorgi et al., 2011), defines hydroclimatic intensity as the product of the mean precipitation intensity and mean annual dry spell length. As such, it does not fall cleanly within our definitions of intensification or acceleration. Increasing HY-INT was a consistent global signature from 1970-2000, indicating higher hydroclimatic intensity (Giorgi et al., 2011). A key strength of HY-INT is that it recognizes the contribution of both dryness and wetness to hydroclimatic intensity. However, the resulting index lacks interpretability and does not measure the coupling of hydrological cycle stages, the goal of this work.

1.1.3 Changes in residence times

Perhaps the most appropriate *existing* characterization of hydrological cycle acceleration is the change in water residence time, or the average length of time water spends in a stage of the hydrological cycle. Shortening residence times indicate hydrological cycle acceleration. Lengthening residence times indicate deceleration. Highlighting the need to distinguish intensification and acceleration, residence times can contradict metrics of hydrological intensification. For example, the residence time of atmospheric water vapor is increasing (deceleration), despite increases in the hydrological fluxes into (E) and out of (P) the atmosphere (intensification) (Bosilovich et al., 2005; Gimeno et al., 2021; Kao et al., 2018; Li et al., 2011). This phenomenon occurs due to a larger increase in E than P.

https://doi.org/10.5194/egusphere-2026-2895
Preprint. Discussion started: 18 June 2026

However, the contrast may not carry over to terrestrial systems. Between 2001-2020, soil water residence time in the top meter of soil water decreased alongside increased P+E, suggesting a coupling of intensification and acceleration (Wang et al., 2023). A key advantage of residence times is that they provide a measure of temporal coupling between hydrological cycle stages. However, this integration is non-specific and combines multiple pathways. For example, soil water residence time cannot distinguish between water that ultimately contributes to streamflow and water that is returned to the atmosphere through evaporation. Furthermore, their calculation over land requires multiple flux and storage variables, introducing uncertainty compared to simpler metrics like WCI. As opposed to more interpretable metrics such as changes in P or even WCI, the implications of changing residence times may be more challenging to communicate to stakeholders such as land managers.

1.2 A novel metric to quantify hydrological cycle acceleration

In response to the lack of a metric of hydrological cycle acceleration that focuses on the explicit coupling of different stages of the hydrological cycle, we introduce a novel metric of hydrological cycle acceleration. In contrast to previous studies that define hydrological cycle acceleration using flux magnitudes (Feng et al., 2017; Huntington et al., 2018; Ohmura and Wild, 2002; Vargas Godoy and Markonis, 2023; Yeh and Wu, 2018) or residence times (Wang et al., 2023), we base our definition of acceleration in the lag component of drought propagation. Drought propagation describes the transfer of deficits—typically measured in anomaly space using drought indices—from meteorological (precipitation) to agricultural (soil moisture) to hydrological (streamflow) (Van Loon et al., 2012). The lag represents the time delay between meteorological drought and subsequent agricultural or hydrological drought. Here, we focus on the lag between meteorological anomalies and subsequent soil moisture anomalies. By including both positive and negative anomalies, rather than drought events alone, we extend the concept of drought propagation to achieve a complete picture of anomaly propagation from atmosphere to land surface. We apply this metric to understand hydrological cycle acceleration over the CONUS domain from 1951-2020, offering a unique contribution to the study of hydrological cycle acceleration and impacts.

2 Materials and methods

We introduce a novel metric of hydrological cycle acceleration based on the response time of a Standardized Soil Moisture Index (SSI) to the Standardized Precipitation Index (SPI) and apply it to understand whether the hydrological cycle has accelerated over CONUS from 1951-2020. The process of calculating time series of SPI and SSI is described in Sect. 2.1. The experimental design for quantifying and comparing response times between the two drought indices is described in Sect. 2.2. A variable importance framework to understand how explanatory hydroclimate variables may influence the response time is outlined in Sect. 2.3. Finally, descriptions of the data used, and additional data processing steps are described in Sect. 2.4.

https://doi.org/10.5194/egusphere-2026-2895
Preprint. Discussion started: 18 June 2026

2.1 Using drought indices to quantify meteorological and soil moisture anomalies

Drought indices provide a standardized framework to monitor and study drought by assigning a numerical value to drought severity (Svoboda and Fuchs, 2016). Typically representing a single type of drought (e.g. meteorological or agricultural), the simplest form of a drought index resembles a standardized anomaly (Z-score) of recent conditions relative to a historical climatology. Many drought indices include a user-chosen accumulation period, allowing conditions to be aggregated over preceding weeks or months to capture drought processes at different temporal scales. We start with the SPI as a measure of meteorological drought (McKee et al., 1993) because drought propagation generally begins with a rainfall deficit (Van Loon et al., 2012). SPI was specifically chosen as it is perhaps the most widely used drought index, given its low data requirements, ease of calculation, and straightforward interpretability. For reference, the World Meteorological Organization has recommended that SPI be the standard meteorological drought index (Hayes et al., 2011).

Daily SPI is calculated at each reanalysis grid cell (see Sect. 2.4 for a description of datasets used) over CONUS following McKee (1993). Precipitation is converted to a daily rolling sum corresponding to the chosen accumulation period. We chose relatively short accumulation periods for SPI to target sub-seasonal to seasonal anomalies rather than multi-seasonal or interannual anomalies. While common accumulation periods for SPI are 1-, 3-, 6-, and 12-months, previous work has demonstrated 1- and 3-month accumulations for SPI correlate most strongly with soil moisture anomalies and reflect the shortest of the common SPI accumulations (Cammalleri et al., 2024). In this analysis, we focus on 30-day and 90-day accumulations (SPI-30 and SPI-90), with the 30-day accumulation of SPI serving as the only accumulation used in most of the analyses in this work (additional justification provided in Sect. 3.1.) For each day of the year, a two-parameter gamma distribution is fit to the historical rolling sums of precipitation on that day of the year using maximum likelihood estimation. Cumulative probabilities of each day's rolling sum of precipitation are retrieved from the gamma distribution and transformed into a standardized score using an inverse normal function.

The choice to use a soil moisture drought index was also based on the accepted order of drought propagation, from meteorological to agricultural (Van Loon et al., 2012). Currently, no broad consensus exists regarding the optimal procedure for calculating a standardized soil moisture index or quantifying anomalies in soil moisture (Cammalleri et al., 2024; Carrão et al., 2016; Hao and AghaKouchak, 2013; Lema et al., 2025; Mo, 2011; Xu et al., 2018). We chose to prioritize consistency and apply the SPI framework to calculate SSI, following the example of Hao and AghaKouchak (2013). A 30-day averaging (replacing accumulation) period is used for the calculation of SSI, to reflect sub-seasonal anomalies, and to match the 30-day accumulation of SPI used as the primary SPI accumulation. To align with previous work analyzing soil water residence time, we calculate SSI for the top meter of soil (Wang et al., 2023). For both SPI and SSI, the total number of full years available at the time of calculation, 1950-2023, are used for fitting the two-parameter gamma probability distributions for precipitation and soil moisture, respectively.

https://doi.org/10.5194/egusphere-2026-2895
Preprint. Discussion started: 18 June 2026

2.2 Experimental design

2.2.1 Quantifying the velocity of the hydrological cycle

The core goal of this paper is to introduce a new approach to quantify acceleration, or changes in velocity, of the hydrological cycle. Recall, we define the velocity as the time it takes hydrological anomalies—as measured through drought indices—to propagate from meteorological anomalies to soil moisture anomalies. We quantify the velocity of anomaly propagation as the response time of SSI to SPI, calculated at a grid cell level using a maximized correlation approach. Specifically, the lag time (SSI-30 lagging behind SPI) that maximizes the Pearson correlation coefficient (***r***) between the two time series is taken as the response time. Similar maximized correlation approaches are well-documented in drought propagation literature (Cammalleri et al., 2024; Jeong et al., 2024; Lema et al., 2025; Zhou et al., 2024). This response time serves as our measure of the velocity of the local hydrological cycle. To avoid issues with frozen soil and snow water storage, we consider only the summer—June, July, August (JJA)—time series of SSI-30 (from here on referred to as JJA SSI-30). An example of how the response time is calculated for a single grid cell for both SPI-90 and SPI-30 is shown in Fig. 1. The shorter, 30-day accumulation period of SPI results in a longer response time and lower correlation at the response time (Fig. 1a, b) as compared to the longer, 90-day accumulation period (Fig. 1c, d). The Pearson correlation was chosen here, although our testing indicates that the choice of Spearman or Pearson correlation results in negligible differences in response time. Short response times indicate that anomalies in SPI are quickly matched by anomalies in SSI, i.e., a *higher velocity* hydrological cycle, and long response times indicate slower propagation—a *lower velocity* hydrological cycle. Thus, a decrease in response time between two time periods represents an accelerating hydrological cycle and vice versa.

https://doi.org/10.5194/egusphere-2026-2895
Preprint. Discussion started: 18 June 2026

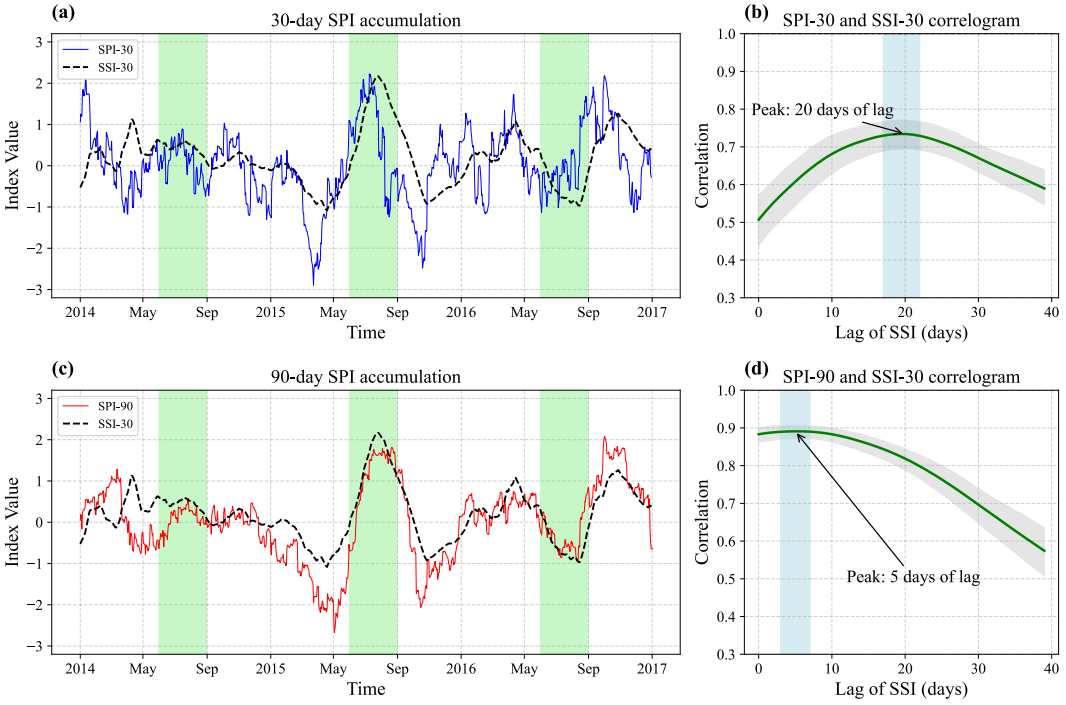

Figure 1: Example calculation of response time between SPI and SSI at 42° N, -84° W. (a) Time series of SPI-30 and SSI-30 from 2014-2016 (note that response time labelled in (b,d) is calculated for full time series, 1951-2020). Green shaded areas represent June, July, and August months for which the response time is calculated. Solid blue line tracks SPI-30 time series, black dashed line tracks SSI-30 time series. (b) Correlogram for SPI-30 and SSI-30 time series showing the correlation coefficient value between SPI-30 and SSI-30 for different lags. Arrow and label mark the lag of SSI-30 that maximizes the correlation between both time series, taken as the response time, or velocity, of hydrological cycle. Blue vertical shaded area represents 95% confidence interval of lag that maximizes correlation. Grey shaded areas represent 95% confidence interval of correlation coefficient values. (c) Same as (a), but for SPI-90 and SSI-30. Solid red line tracks SPI-90 time series. (d) Same as (b), but for SPI-90 and SSI-30. Data is from ERA5-Land, with a more detailed description in Sect. 2.4.

To understand the spatial distribution of response time of SSI-30 to SPI (both SPI-30 and SPI-90) across CONUS, we calculate a response time during the period 1951-2020 at every grid cell for the SSI-30 time series. Only lags of up to 300 days are tested, and response times are calculated beginning in 1951 to allow for SPI lags of up to 300 days.

2.2.2 Bootstrapping to assess significance of correlation peak at response time

We assess the significance of the correlation peak at each grid cell's calculated response time (Sect. 2.2.1) by testing whether its ***r***-value significantly exceeds the ***r***-value at zero days of lag. Following the approach of Efron and Tibshirani (1994), a moving blocks bootstrapping approach is used to address autocorrelation present in the time series. Moving block bootstrapping considers contiguous blocks of a chosen time length as candidates for resampling, rather than individual data points (i.e., individual days). Since we only analyze the JJA (three months per year) time series of SSI-30, we employ an equivalent block size of three months to ensure functional independence between blocks. We generate 1000 resampled (with replacement) time series from the original JJA SSI-30 time series, with

https://doi.org/10.5194/egusphere-2026-2895
Preprint. Discussion started: 18 June 2026

1000 chosen to stabilize resulting bootstrapped distributions (Efron and Tibshirani, 1994). Computing the correlation with the SPI times series at zero lag for all 1000 resamples allows for the construction of a one-sided 95% confidence interval around the ***r*** value at zero lag. The null hypothesis (H_0) that the ***r*** at the response time is not significantly different from zero lag ***r*** is rejected (significance achieved at $\alpha = 0.05$) if the ***r*** at the response time falls outside this interval.

2.2.3 Quantifying the acceleration of the hydrological cycle

We primarily assess the long-term acceleration of the hydrological cycle through the change in response time between an early (1951-1985) and late (1986-2020) time period. For each grid cell, we calculate response time between SPI-30 and JJA SSI-30 (Sect. 2.2.1) for both time periods. A decrease in response time in the late time period relative to the early time period indicates an acceleration of the hydrological cycle.

We evaluate significant changes in response time using a moving blocks bootstrap approach, with the same 3-month block size and number of resamples (1000) as in Sect. 2.2.2. Here, only the early time period is resampled, and a bootstrapped distribution of 1000 resampled response times is generated using resampled SSI time series and the SPI time series. For each grid cell, the calculated response time in the later period is compared against this bootstrapped distribution of response times to generate one p-value per grid cell, representing the result of a two-sided hypothesis test with an H_0 of no change in response time from early to late period (Efron and Tibshirani, 1994). We apply the false discovery rate (FDR) procedure (Benjamini and Hochberg, 1995), outlined in S1, to the set of significance tests to account for the multiple comparison test problem. This problem arises when many individual (local) hypothesis tests are conducted, which can result in many Type 1 errors (i.e., incorrectly rejected H_0). The FDR procedure limits the rate of Type 1 errors. Here, we use $\alpha_{FDR} = 0.05$, which limits the expected rate of Type 1 errors to 5% of the total number of rejected local null hypotheses (Benjamini and Hochberg, 1995; Wilks, 2016, 2019).

We recognize that shorter-term variability may be important and present a secondary analysis in which we investigate regional changes in response time at a decadal time scale to test how robust observed changes are to choices in time period and spatial scale. We aggregate total precipitation and volumetric soil water content in the top one meter of soil across the nine climate regions defined by the National Center for Environmental Information (NCEI) (Karl and Koss, 1984), resulting in nine time series of regional daily total precipitation and soil moisture. Daily regional SPI-30 and JJA SSI-30 values are calculated for each region (Sect. 2.2.1), and the response time of JJA SSI-30 to SPI-30 is calculated by decade for each region.

2.3 Evaluating the role of hydroclimate variables on changes in response time

The roles of different hydroclimatic variables on response times are investigated with a Random Forest (RF) regression (Breiman, 2001). RF regression was chosen for its ability to capture non-linearities and integrate complex relationships among variables while reducing overfitting (Zhang and Ma, 2012). We fit two RF models to identify hydroclimate drivers of response times across CONUS during the period 1951-2020, using predictors from ERA5-Land (Tables 1 and 2). We employ permutation importance to evaluate which variables drive prediction skill, while partial dependence plots visualize the marginal effect of the most important variables on predicted response time.

https://doi.org/10.5194/egusphere-2026-2895
Preprint. Discussion started: 18 June 2026

2.3.1 Random Forest (RF) fitting

The RF algorithm and hyperparameters are described in S2. Both of our RF models consisted of 1000 trees with a maximum depth of 10, considering one-third of predictor variables at each split. The resulting RF can predict response times at grid cells based on these predictors, however we use it to evaluate variable importance. Thus, predictions are done only to evaluate model performance on test data.

The first model is trained on variables (Table 1) chosen to represent the water inputs to the land surface (precipitation), while E and potential evapotranspiration (PET) represent atmospheric demand. Temperature (T) serves as a general climate indicator. All variables are considered as both annual and seasonal averages to determine if specific seasons disproportionately influence summer response times. The seasonal divisions used are MAM (March, April, May), JJA (June, July, August), SON (September, October, November), and DJF (December, January, February). Additionally, the seasonal percentage of annual precipitation and evaporation is included as another indicator of seasonality.

Table 1: Representative variables and clusters for single-variable random forest regression. The random forest models are trained using the representative variables (left-hand column), which are chosen to represent the effect of some grouping of correlated variables (right-hand column). Except where noted as percentages, all variables are annual or seasonal means.

Representative variable	Other variables included in cluster (if applicable)
Percent P in MAM	
Percent E in MAM	
Percent P in SON	
Percent E in SON	
Summer mean temp	
P in DJF	
Annual soil moisture	Soil moisture in MAM, JJA, SON, and DJF (all were highly correlated)
Annual E	E in SON, E in MAM
P in JJA	E in JJA
Annual P	P in MAM, P in SON
Annual PET	PET in MAM, JJA, SON, and DJF (all were highly correlated)
Annual T	E in DJF, soil moisture in MAM, JJA, SON, and DJF (all were highly correlated)
Percent E in JJA	Percent of E in DJF

The second RF model is trained on hydroclimatic variables derived from ERA5-Land outputs (Table 2). We chose P+E to analyze the relationship between response time and the WCI (Huntington et al., 2018), while P-E serves an indicator of both the atmospheric and terrestrial water budget (Bosilovich et al., 2005). Including an aridity index (PET/P) (Budyko and Miller, 1974) allows us to understand the potential effect of aridity on response times. The residence time of soil water (RT) serves as a terrestrial analogue for the atmospheric hydrological cycle velocity (Wang et al., 2023). Equation 2 describes the residence time calculation (Wang et al., 2023), where P is total precipitation and S is the average soil moisture in the top meter of soil for a given period of time:

$$RT = \mathrm{S/P} \qquad (2)$$

The calculation of residence time using a volume (S) and flux (P) assumes a steady state and mass conservative system, making it an approximation of the true residence time.

https://doi.org/10.5194/egusphere-2026-2895
Preprint. Discussion started: 18 June 2026

Table 2: Representative variables and clusters for random forest regression model built on derived, multi-variate hydroclimatic indicators. The random forest models are trained using the representative variables (left-hand column), which are chosen to represent the effect of some grouping of correlated variables (right-hand column). All variables are annual or seasonal means.

Representative variable	Other variables included in cluster (if applicable)
PET/P in DJF	
P-E in JJA	
P+E in DJF	RT in DJF
Annual PET/P	PET/P in MAM, SON
Annual RT	RT in MAM, SON
Annual P+E	P+E in MAM, SON
P+E in JJA	PET/P in JJA, RT in JJA
Annual P-E	P-E in MAM, SON, DJF

The performance of both RF models is measured through R^2, using a standard 5-fold cross-validation approach (Hastie et al., 2009). We adjust the 5-fold cross validation to include a spatial-blocking approach (procedure described in S5) to minimize the impact of spatial overfitting in performance metrics (Roberts et al., 2017; Valavi et al., 2018).

2.3.2 Assessing influence of hydroclimatic variables on response time

We identify potential hydroclimatic drivers of our novel metric of hydrological cycle velocity—response time of JJA SSI-30 to SPI—by calculating the permutation importance (Zhang and Ma, 2012) of hydroclimatic predictor variables. As opposed to common impurity based metrics (Hastie et al., 2009), permutation importance measures a variable's influence in the prediction of unseen test data rather than its importance in model training. After training an RF regression on each of the five training datasets (Sect. 2.3.1), we measured the predictive performance (R^2) against the complementary test datasets. The decline in predictive performance after randomly permuting a variable—while keeping all other variables fixed—is the permutation importance score. Permuting important variables should decrease predictive performance more than unimportant variables. We permute each variable 10 times, calculating a median (Pedregosa et al., 2011) permutation importance score for each variable in each training/testing split. The resulting set of 5 median permutation importance scores per variable is used to assess variable importance.

Because correlated variables can 'share' variable importance and obscure drivers of predictive skill (Zhang and Ma, 2012), we follow a solution outlined by the creators of the Python predictive data science package, *scikit-learn* (Pedregosa et al., 2011). The procedure, outlined in S3, hierarchically clusters variables and retains one variable from each cluster to represent the effect of that cluster (Tables 1 and 2). The RF regression is trained using only those representative variables. Importance is assigned to the representative variable (and implicitly, the cluster).

2.3.3 Visualizing partial dependence of response time on hydroclimatic variables

Partial dependence plots (PDPs) illustrate the interaction between response time and the top four most important variables for each model. A PDP for variable $\boldsymbol{X}$ visualizes how the average predicted response time varies along with

https://doi.org/10.5194/egusphere-2026-2895
Preprint. Discussion started: 18 June 2026

varying values of $\boldsymbol{X}$. The algorithm to produce PDPs is described in S4. Due to the multi-dimensional interactions captured by an RF, the resulting PDP visualization is simply an average, and not a deterministic measure of how predicted response times vary with varying values of $\boldsymbol{X}$ in every scenario.

2.4 Reanalysis data used to calculate drought indices and analyze variable importance

The primary categories of hydroclimate data needed for this study are atmospheric (P, T, PET, E) and land surface (soil moisture to a depth of one meter). These data serve as inputs for calculating drought indices and the RF regression analysis. While using observational data may be ideal, these datasets often suffer from limited spatial and temporal coverage, particularly for key states and fluxes such as soil moisture and evapotranspiration. To ensure physical consistency across all variables, we use reanalysis data for all data inputs. Reanalysis data effectively bridges the gap between purely observational and purely modeled datasets by assimilating observations into a physically based model. The ERA5-Land reanalysis, available through the European Centre for Medium Range Weather Forecasting (ECMWF), is chosen as a physically consistent reanalysis constrained to observations, with coverage from 1950 to present and soil moisture at depths of up to 2 meters (Muñoz-Sabater et al., 2021). ERA5-Land was chosen due to its relatively fine spatial resolution (gridded to 0.1°, with a native resolution of 9 km) and lengthy temporal coverage (1950-present) compared to other hydroclimatic datasets. ERA5-Land consists of a land surface model (H-TESSEL) forced with downscaled ERA5 outputs (Hersbach et al., 2020). The downscaled ERA5 precipitation is used extensively in this analysis. ERA5 temperature and precipitation exhibit high correlations with observations across Canada and CONUS and perform comparably to observation-based datasets when used as forcing for hydrological models, achieving median KGE scores of approximately 0.75 across 3,138 catchments (Tarek et al., 2020). As ERA5 has no direct assimilation of precipitation observations pre-1979 (Bell et al., 2021), precipitation outputs may have reduced reliability pre-1979. The evapotranspiration, PET, and soil moisture terms used here are entirely model-derived in ERA5-Land, with no assimilation of observational data. Validation of ERA5-Land soil moisture against in-situ observations over North America shows acceptable skill (Muñoz-Sabater et al., 2021). Comparison studies show ERA5-Land to have comparable or superior soil moisture skill to other reanalysis products (Beck et al., 2021; Zheng et al., 2024). Validations of ERA5-Land evapotranspiration and potential evapotranspiration are limited in quantity and study area. Jin et al. (2024) compared four evapotranspiration products to an 'actual terrestrial evapotranspiration dataset' developed using the complementary evapotranspiration method. ERA5-Land performed best, with correlation coefficients exceeding 0.96. A separate evaluation of ERA5-Land PET over mainland China found ERA5-Land to have mean correlation coefficients of 0.75 when compared to observed pan evaporation (Xu et al., 2024). PET in ERA5-Land is computed as open water evaporation using the bulk aerodynamic method (ECMWF, 2025).

https://doi.org/10.5194/egusphere-2026-2895
Preprint. Discussion started: 18 June 2026

3 Results

3.1 Distribution of response times across CONUS

We report the distribution of response times of JJA SSI-30 to both SPI-30 and SPI-90 across CONUS to explore how response time varies spatially across CONUS and between different SPI accumulations (Fig. 2a,d). Using the maximized correlation approach (Sec. 2.2.1), response times of JJA SSI-30 to both SPI accumulations ranged from zero days to the maximum tested response time, 300 days. For reference, Fig. S1 shows a histogram of the response times for each accumulation. However, the mean (median shown in parentheses) response times for SPI-90 and SPI-30 were 38 (17) days and 24 (4) days, respectively (Fig. S1). Spatial patterns of response times were generally similar between both accumulations of SPI. Shorter response times prevailed in the eastern half of the domain, on the order of 10-20 days for SPI-30 and 0-10 days for SPI-90. Longer response times dominated in the western US, with response times exceeding 100 days in much of the southwest and parts of the northwest.

The correlation between JJA SSI-30 and SPI also showed similar patterns between the two accumulations of SPI (Fig. 2b,e). The highest correlations were in the eastern half of the domain, greater than 0.8 for SPI-90 and between 0.6 and 0.8 for SPI-30. Correlation coefficients were consistently smaller in the west, with most grid cells falling between 0.6 to 0.8 for SPI-90 and 0.4-0.6 for SPI-30. Patterns of correlation and response time appeared to have an inverse relationship: longer response times were associated with lower peak correlations. We conducted local one-sided significance tests (α=0.05) at the grid cell level to test whether the peak correlation (at the calculated response time) was significantly greater than the correlation at no lead time for SPI (Fig. 2c,f). Over 93% of grid cells had significant peaks for SPI-30, as opposed to under 14% for SPI-90. Given that negative lags of SSI-30 were not considered, the presence of a defined peak at a non-zero response time is essential to analyzing both hydrological cycle acceleration and deceleration across CONUS. As only a low percentage of grid cells showed a significant non-zero peak for SPI-90 (Fig. 2f), SPI-30 is used in subsequent analyses to allow for an exploration of both acceleration and deceleration. Although using SPI-30 comes at the cost of lower overall correlations, we believe the tradeoff is necessary.

https://doi.org/10.5194/egusphere-2026-2895
Preprint. Discussion started: 18 June 2026

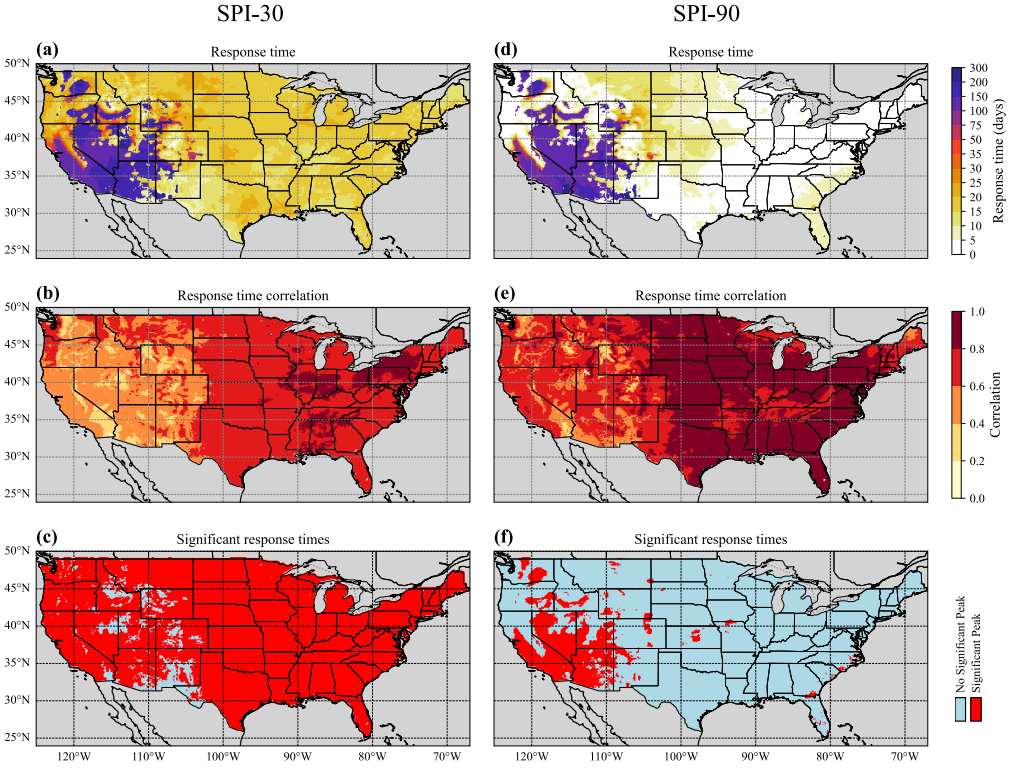

Figure 2: Distribution of response times between SPI and summer (JJA) SSI-30 across CONUS for the time period 1951-2020 using ERA5-Land data. (a) Response times between SPI-30 and SSI-30, calculated by a maximized correlation approach between the two time series. (b) Pearson's correlation coefficient between JJA SSI-30 and lagged SPI-30 for the calculated response time. (c) Significance of the correlation peak at the response time. Significance of the peak is determined by calculating whether correlation at peak is significantly different (α=0.05) from the correlation between the unlagged time series, using a moving blocks bootstrap approach. (d-f) same as (a-c), but for SPI-90 and SSI-30. Procedures used to generate plots can be found in Sect 2.2.1 and 2.2.2, while a description of data used can be found in Sect. 2.4.

3.2 Influence of hydroclimatic variables on response time

We evaluated potential individual hydroclimatic drivers of response time of JJA SSI-30 to SPI-30 through permutation importance analysis of an RF regression model, shown in Fig. 3. To limit the impact of highly correlated variables on the permutation importance measurements, we used representative variables from variable clusters when building the model (Table 1). The median R^2 value from 5-fold spatially blocked cross-validation was 0.83, indicating adequate model performance to assess variable importance. We identified the four most important representative variables, each representing one variable cluster (see Sect. 2.3.1 and Table 1), ranked by median permutation importance scores across 10 members and 5 cross-validation test sets. The most important representative variable was mean annual precipitation (variable cluster also includes mean SON and MAM precipitation), followed by mean JJA precipitation (variable cluster also includes mean JJA evaporation), mean annual evaporation (variable cluster also includes mean SON and MAM evaporation), and mean DJF precipitation (not clustered with any other variable). Mean DJF precipitation was substantially less important than the top three. Median R^2 drops of the top three variables were between 0.13 and 0.28,

https://doi.org/10.5194/egusphere-2026-2895
Preprint. Discussion started: 18 June 2026

while all other variables had a median R^2 drop below 0.05 (Fig. 3b). Partial dependence plots indicated that the marginal relationship between response time and the top three variables was negative (left three plots of Fig. 3c), meaning higher levels of mean annual precipitation, mean JJA precipitation, and mean annual evaporation result in lower predicted response times. The relationships were non-linear, with sharp changes in response times occurring at the lower end of changes to variable values, as shown in the left-hand portion of the panels of Fig. 3c.

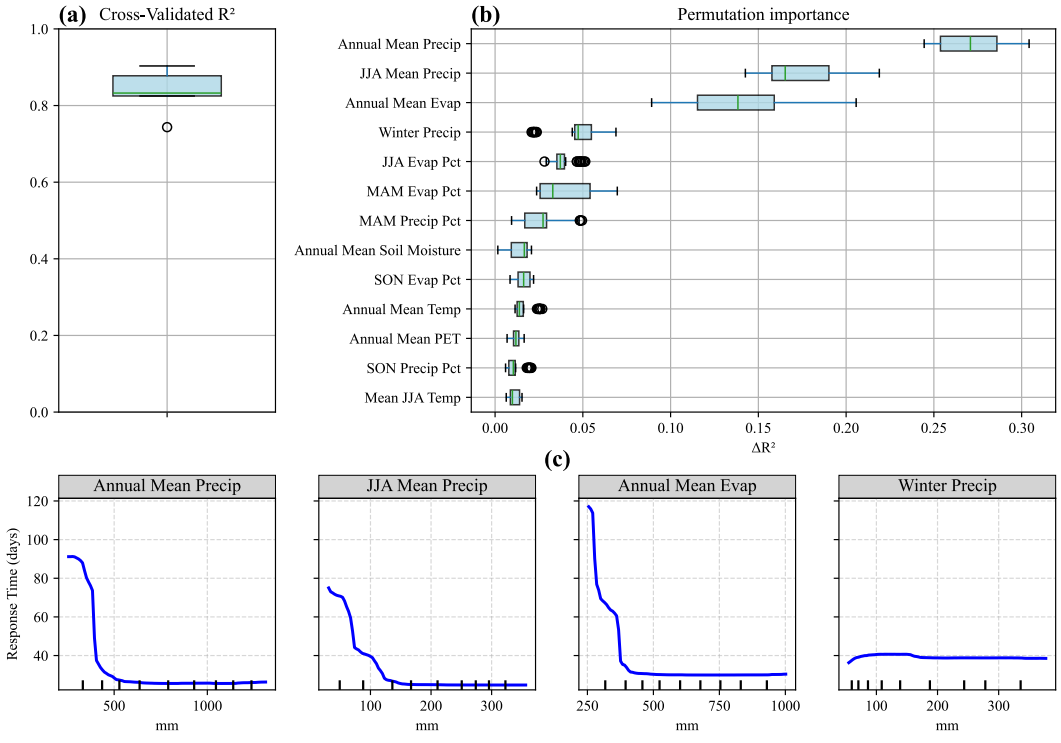

Figure 3: Random Forest model performance, variable importance, and partial dependence plots for individual hydroclimatic variables. RF model was trained to predict the response time of JJA SSI-30 to SPI-30 in the time period 1951-2020 given a set of hydroclimatic variables downloaded from ERA5-Land data. (a) Predictive skill of the RF, measured through the R^2 of predicted vs. observed response time in each of the 5 test datasets produced by 5-fold spatially blocked cross-validation. Median R^2 was 0.83. (b) Permutation importance score for the representative variables used to build the RF. ΔR^2 refers to the drop in predictive skill of the model on testing data when a given variable is permuted. Boxplots represent the distribution of ΔR^2 across the 5 test datasets, with 10 permutations per variable, giving 50 ΔR^2 scores per variable. (c) Partial dependence plots of the top four variables, representing the average marginal dependence of response time on each of the top four variables. Data is from ERA5-Land, with a more detailed description in Sect. 2.3 and 2.4.

A second RF regression analyzed the importance and influence of derived multivariate hydroclimatic variables on the response time, shown in Fig. 4. A separate model avoids distributing importance between derived hydrological variables and their original components (such as P and P+E). As many of the multivariate hydroclimatic variables are often used as indicators of hydrological velocity (see Sect. 1.1), this model allows a comparison between response time and those metrics. The multi-variable model performed similarly to the single-variable model, with a median R^2 value of 0.80 across 5-fold spatially blocked cross-validation. Permutation importance identified JJA mean P+E

https://doi.org/10.5194/egusphere-2026-2895
Preprint. Discussion started: 18 June 2026

(representative of mean JJA PET/P and mean JJA soil water residence time), annual mean P+E (representative of SON and MAM mean P+E), annual mean P-E (representative of MAM, SON, and DJF mean P-E), and winter mean P+E (representative of DJF soil water residence time) as the most influential variables. The JJA mean P+E and annual mean P+E had median R^2 drops of 0.40 and 0.20 respectively. No other variable had a median R^2 drop above 0.1. Like the partial dependence in the single-variable model, the influence of the top three variables was negative, meaning higher levels of JJA mean P+E, annual mean P+E, and annual mean P-E result in lower predicted response times while winter mean P+E had no clear relationship. This indicates that larger flux magnitudes here (and in Fig. 3c), correspond with a higher velocity hydrological cycle. The relationships were again non-linear, with sharp changes in response times occurring at the lower end of changes to variable values.

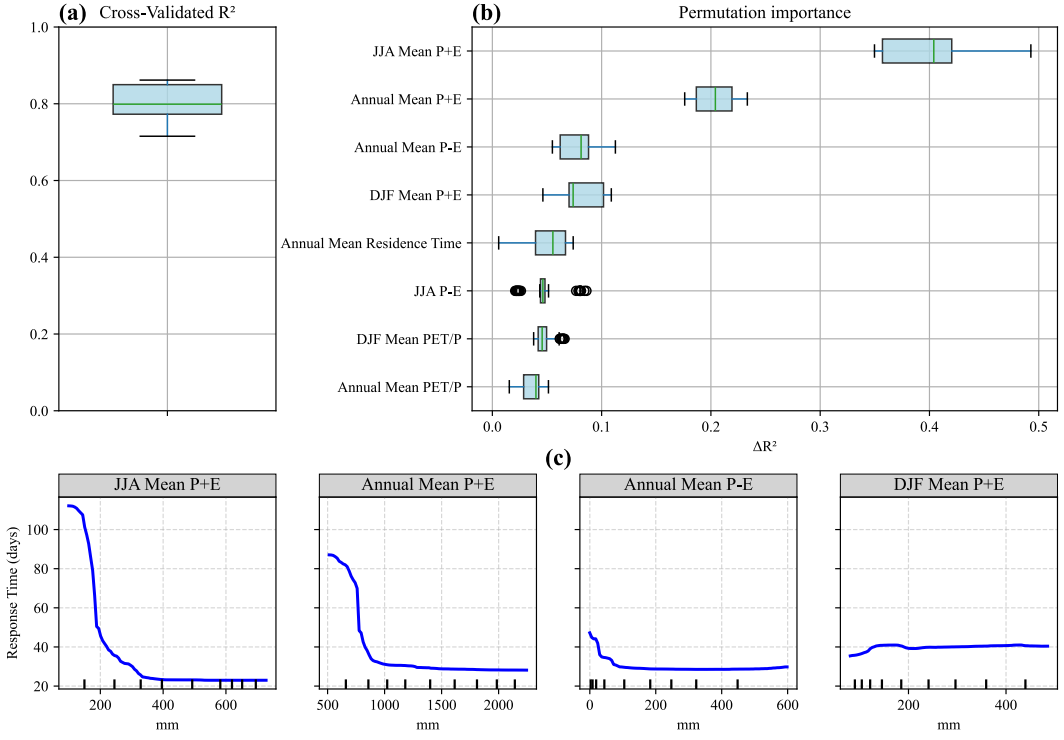

Figure 4: Random forest model performance, variable importance, and partial dependence plots for multi-variable hydroclimatic variables. RF model was trained to predict the response time of JJA SSI-30 to SPI-30 in the full time period 1951-2020 given a set of multi-variable hydroclimatic variables derived from ERA5-Land data. (a) Predictive skill of the RF, measured through the R^2 of predicted vs. observed response time in each of the 5 test datasets produced by 5-fold spatially blocked cross-validation. Median R^2 was 0.80. (b) Permutation importance score for the representative variables used to build the RF. ΔR^2 refers to the drop in predictive skill of the model on testing data when a given variable is permuted. Boxplots represent the distribution of ΔR^2 across the 5 test datasets, with 10 permutations per variable, giving 50 ΔR^2 scores per variable. (c) Partial dependence plots of the top four variables, representing the average marginal dependence of response time on each of the top four variables. Data is from ERA5-Land, with a more detailed description in Sect. 2.3 and 2.4.

https://doi.org/10.5194/egusphere-2026-2895
Preprint. Discussion started: 18 June 2026

3.3 Analyzing hydrological cycle acceleration between an early and late period

We calculated the change in response time between SPI-30 and JJA SSI-30 from an early to late time period (see Sect. 2.2.2) to investigate potential hydrological cycle acceleration/deceleration between 1951-2020 (Fig. 5a-b). As defined earlier, a decrease in the response time denotes an accelerating hydrological cycle, i.e., quicker anomaly propagation, while an increase denotes a decelerating hydrological cycle, i.e., slower anomaly propagation. The significance of the change in response time is also reported, both before the FDR correction (Fig. 5c, α=0.05), and after the FDR correction (Fig. 5d, α_{FDR}=0.05). More grid cells experienced an increase in response time (deceleration): 48.47% of grid cells. Grid cells with decreased response time (acceleration) comprised 39.32% of the data. Overall, 12.21% of grid cells had no change in response time. The central and northern Great Plains experienced the most spatially coherent acceleration, along with central Texas and the mid-Atlantic coast (Fig. 5b). The most coherent regions of deceleration were in much of the northern Midwest, South, and west coast of CONUS (Fig. 5b). While pockets of the observed accelerations and decelerations were deemed significant prior to the FDR correction (Fig. 5c), no CONUS grid cells were found to have a significant acceleration or deceleration after applying the FDR procedure (Fig. 5d). As opposed to relatively coherent areas of increasing and decreasing response times found in eastern and central CONUS, changes in response times across southwestern and western CONUS were noisy (Fig. 5b). Small areas of large coherent change in both directions were found, but meaningful signals were difficult to separate from apparent noise. This western US region, which is known for extremes in hydroclimate, had both the longest response times (100-200 days) and the largest changes in response time. Increases and decreases greater than 35 days occurred in close proximity.

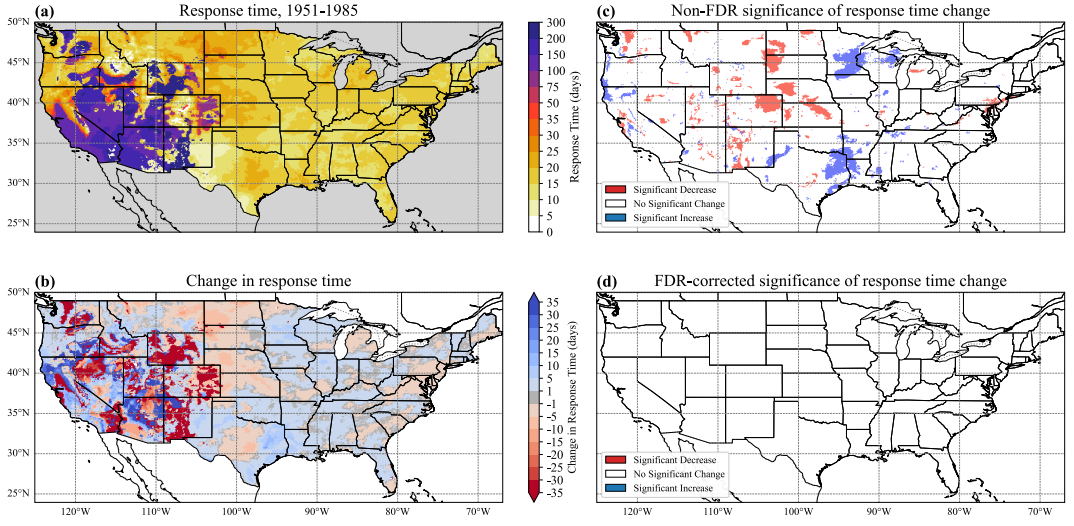

Figure 5: Change in response time of JJA SSI-30 to SPI-30 across CONUS between time periods 1951-1985 and 1986-2020. (a) Response time calculated for early time period (1951-1985). (b) Change in response time from early to late period. 48.47% of grid cells had an increased response time, 39.32% had decreased response time, 12.21% had no change in response time. (c) Areas with significant increases or significant decreases in response time between periods (α=0.05), prior

https://doi.org/10.5194/egusphere-2026-2895
Preprint. Discussion started: 18 June 2026

to FDR correction. 5.25% of grid cells had a significant increase in response time, 5.49% had a significant decrease, and 89.26% had no significant change in response time. Significance measured by comparing response time in 1986-2020 to two one-sided confidence intervals around the response time from 1951-1985. Confidence intervals were generated using a moving blocks bootstrap. (d) No areas showed significant increases or significant decreases in response time between periods after FDR correction (α_{FDR}=0.05). Significance calculated in the same manner as (c), but with FDR procedure (Sect. 2.2.3) applied. Data is from ERA5-Land, with a more detailed description in Sect. 2.4.

3.4 Regional trends in response time

We analyzed decadal trends in response time from 1951 to 2020 by NCEI climate region to understand whether local trends in response time translated into regional signals (Fig. 6). Mann-Kendall testing revealed no significant trend in any of the regions, with the smallest p-value being ~0.22 for the positive trend in response time in the Northwest. While the low sample size (n=7) of decadal response times per region limits the power of the significance test to detect a trend, Mann-Kendall testing using 5-year intervals (not shown) also identified no statistically significant regional trend.

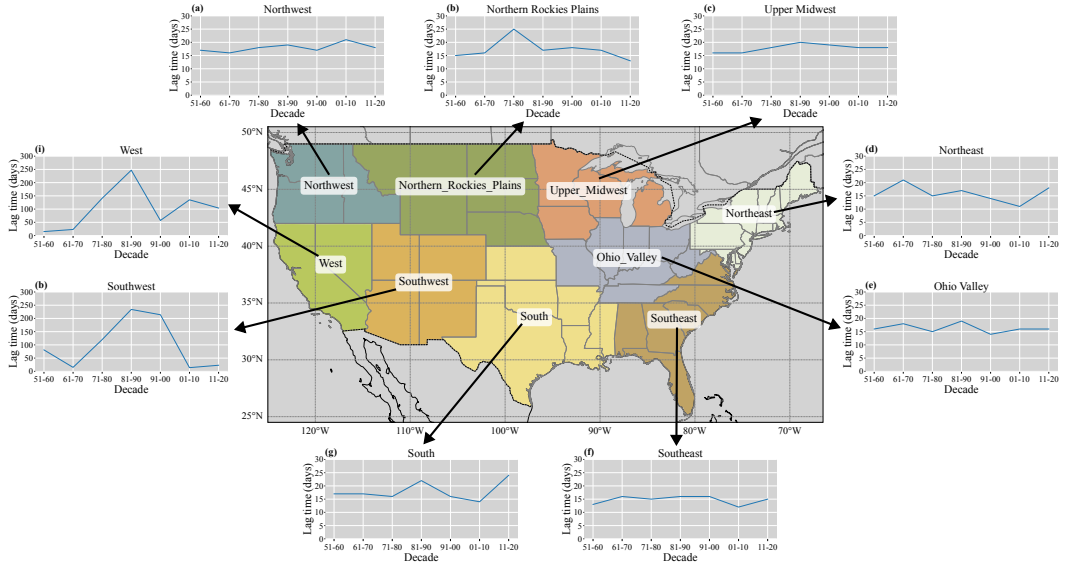

Figure 6: Decadal variation in response time by NCEI climate region from 1951-2020. Response times are the response of JJA SSI-30 to SPI-30. SPI and SSI time series were generated by averaging daily precipitation and soil moisture across individual regions and then applying SPI framework to resulting time series. Central map shows NCEI climate regions and CONUS state borders. Arrows point from NCEI regions to corresponding line plots of decadal changes in response time. Clockwise from top left, regions are (a)Northwest, (b)Northern Rockies and Plains, (c)Upper Midwest, (d)Northeast, (e)Ohio Valley, (f)Southeast, (g)South, (h)Southwest, (i)West. Data is from ERA5-Land, with a more detailed description in Sect. 2.4.

The West and Southwest NCEI regions (Fig. 6h and 6i) exhibit large increases in decadal response time between 1971-2000, but no significant monotonic trend. Although the mechanisms driving these increases are not fully explored in this study, they may be related to the structure of the correlograms in these regions (Fig. 7a-d). These correlograms are characterized by relatively flat shapes with less prominent and lower peaks in correlation than other regions (e.g. Fig. 7b vs 7f), and multiple local maxima at similar correlation values (Fig. 7b-d). Together, these features suggest that summer soil moisture anomalies in the West and Southwest are weakly dependent on precipitation anomalies at

https://doi.org/10.5194/egusphere-2026-2895
Preprint. Discussion started: 18 June 2026

any single lag time and instead reflect modest correlations across a broad range of lag times. Under such conditions, small shifts in precipitation patterns (e.g. sequences of wet or dry winters) may result in large apparent changes in decadal response time.

This sensitivity is illustrated in the Southwest, where the estimated response time shifted from 234 days in 1981-1990 to 14 days in 2001-2010 (Fig. 7a,b). In both decades, a local correlation peak occurs at a lag of 14 days, with only a modest increase in correlation from 1981-1990 ($\boldsymbol{r}$=0.44) to 2001-2010 ($\boldsymbol{r}$=0.532). However, the second prominent peak in correlation at longer lag time decreased in both magnitude and timing from $\boldsymbol{r}$=0.65 at 234 days of lag in 1981-1990 to r=0.53 at 142 days of lag in 2001-2010. The relatively small changes in the correlation at both peaks nonetheless produce a large shift in response time from 234 days to 14 days. Although the timing of the second peak does shift from 243 days in 1981-1990 to 142 days in 2001-2010, the calculated shift in response time instead reflects a shift between local peaks rather than the shift in the timing of a local peak. As a result, large decadal changes in response time may arise from subtle changes in correlation structure rather than the specific type of change in hydrological cycle velocity that this metric was designed to capture, limiting the utility of response time as a robust indicator of hydrological cycle velocity in the West and Southwest.

In contrast, the relationship between SPI-30 and JJA SSI-30 in eastern part of the domain is characterized by shorter response times and clear, prominent peaks in correlation (Fig. 7d,f). Although some decades in eastern CONUS showed evidence of a second local peak at higher lag times (Fig. 7f, peak at 276 days), the relative prominence of the primary peak (Fig. 7f, peak at 18 days) provides us with more confidence in the response time as a metric of hydrological cycle velocity in these regions.

https://doi.org/10.5194/egusphere-2026-2895
Preprint. Discussion started: 18 June 2026

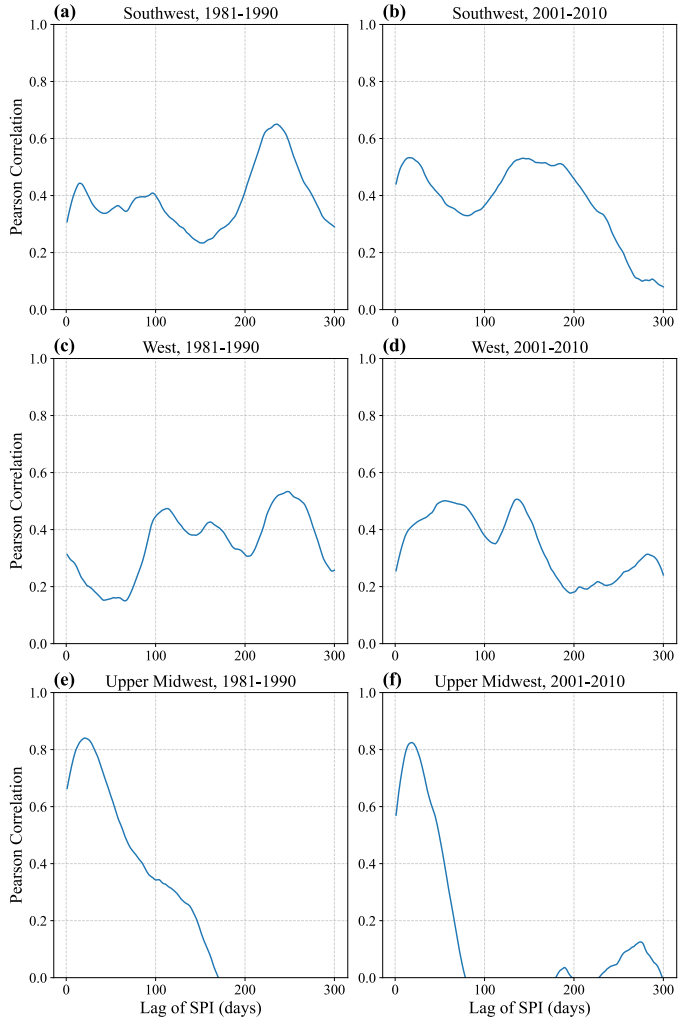

Figure 7: Correlograms in the Southwest, West, and Upper Midwest NCEI climate divisions for two decades: 1981-1990 and 2001-2010. Correlograms display the correlations of SPI-30 and SSI-30 time series at different lags of SPI-30 for given NCEI climate regions. The peak of the correlogram is used as the response time between the two time series. Correlograms for two decades are displayed: (a) Southwest, 1981-1990, response time 234 days), (b) Southwest, 2001-2010, response time of 14 days, (c) West, 1981-1990, response time of 247 days, (d) West, 2001-2010, response time of 135 days, (e) Upper Midwest, 1981-1990, response time of 20 days, (f) Upper Midwest, 2001-2010, response time of 18 days. Correlation refers to the r between the JJA time series of SSI-30 and various lagged time series of SPI-30. 1981-1990 was selected as it is the decade with the highest response times in the West and Southwest. 2001-2010 was chosen as the decade both the West and Southwest return to shorter response times. Data is from ERA5-Land, with a more detailed description in Sect. 2.4.

4 Discussion

The central tendency of response times of JJA SSI to SPI-30 across CONUS were longer than the response to SPI-90, with respective median response times of 17 and 4 days (Fig. 2a, 2d). Response times displayed spatial variability for both accumulations of SPI, with large response times exceeding 100 days found in southwestern CONUS, and much

https://doi.org/10.5194/egusphere-2026-2895
Preprint. Discussion started: 18 June 2026

shorter response times in eastern CONUS. In general, longer response times were associated with lower correlations and less prominent peaks in correlation at the response time. Although Cammalleri et al. (2024) only tested lags of one or multiple dekads (10-day periods), our results align in two key ways: (i) shorter accumulations of SPI obtain maximized correlation with soil moisture drought indices at longer lag times, and (ii) SPI-90 generally results in higher maximum correlations across CONUS. Gevaert et al. (2018) used a different procedure to calculate a drought propagation time, but also found much longer propagation times between SPI and SSI for summer droughts in southwestern and western CONUS. Despite the higher correlations found when using SPI-90 (Fig. 2b,e), we used SPI-30 for subsequent analyses because of the large area with a significant non-zero response time.

4.1 Influence of flux magnitudes on response time

We built two RF models to examine the potential influence of hydroclimate variables on the response time between SPI-30 and SSI-30 (Figs. 3 and 4). We are not aware of any studies that have previously explored explanatory factors for the response time observed between SPI and SSI, although several studies have analyzed potential controlling factors in propagation dynamics between SPI and other forms of drought (Barker et al., 2016; Gevaert et al., 2018). Our single-variable RF analysis (Fig. 3) revealed that the group of variables represented by the mean annual precipitation was the most important to explaining differences in model skill, followed by JJA mean precipitation and annual mean evaporation (Fig. 3b). Partial dependence plots (Fig. 3c) showed that the marginal relationship between all three of those top variables and response time was negative, meaning the RF model predicted lower response times as their values increased. This aligns with studies on drought propagation dynamics from meteorological drought to hydrological drought (as opposed to soil moisture drought studied here), which have found that wetter areas have shorter drought propagation times (Barker et al., 2016; Gevaert et al., 2018). The partial dependence plot for all three variables was non-linear (Fig. 3c), with the most change seen at lower values. This finding implies that measures of wetness may be tied to the large-scale regional differences in response time, such as those seen between the arid southwest and the rest of the domain.

In the RF regression trained on derived multivariate hydroclimatic variables (Fig. 4), the group of variables represented by JJA P+E was by far the most important in terms of model skill, followed by mean annual P+E (Fig. 4b). Higher rates of P+E were associated with lower response times (Fig. 4c). The slope of the summer P+E curve was non-linear (Fig. 4c), albeit with a slightly gentler transition between high response times and lower response times than seen for annual mean precipitation in the single-variable model (Fig. 3b). While we found no clear parallels in the literature to an analysis of the relationship of P+E and drought propagation characteristics, it is not surprising that relationships that exist between response times and precipitation would carry over into relationships of response time and P+E.

A potential explanation for the strong association between higher flux magnitudes and lower response times may lie in soil moisture physics. The state of soil moisture is determined by two processes: wetting and drying. The wetting process occurs more rapidly than the drying process (McColl et al., 2017b). Within the drydown process, the rate of drying is highest initially, and decreases over time (McColl et al., 2017a; Rondinelli et al., 2015; Shellito et al., 2016). Combined with the knowledge that dry soil moisture anomalies tend to persist longer than wet soil moisture anomalies (Brubaker and Entekhabi, 1996), it follows that response times in wet regions will be shorter than response times in

https://doi.org/10.5194/egusphere-2026-2895
Preprint. Discussion started: 18 June 2026

dry regions. In wet areas, the relationship between precipitation and soil moisture will likely depend more on wetting events and the earlier (quicker) phases of drydown (Livneh et al., 2024). Conversely, the relationship in dry areas will depend less on wetting events, and more on the (slower) tail of the drydown curve given their greater prevalence. This would result in a longer response time of anomalies in soil moisture to anomalies in precipitation.

4.2 Changing velocity of the hydrological cycle

We analyzed accelerations and decelerations of the hydrological cycle over CONUS by calculating the difference in response time of SSI-30 (JJA time series only) to SPI-30 between 1951-1985 and 1986-2020 (Fig. 5). Overall, a slightly larger proportion of CONUS grid cells experienced a deceleration (48.47 %) in their hydrological cycle than acceleration (39.32 %). However, after applying the FDR procedure to local significance tests, no grid cells were shown to have experienced a significant acceleration or deceleration in their hydrological cycle between the two periods. This is in contrast to recent studies investigating hydrological cycle acceleration over land, which have found substantially larger percentages of area experiencing acceleration than deceleration (Feng et al., 2017; Wang et al., 2023). However, these studies did not conduct a false discovery correction procedure and were also performed at a global scale and analyzed shorter, more recent time periods, making their conclusions not directly comparable to ours. We did not calculate a mean change across grid cells due to the large spatial variability in both overall response times and changes in response time. We found spatially coherent areas of hydrological cycle acceleration in the Great Plains and mid-Atlantic, and spatially coherent areas of deceleration in the Upper Midwest, South and West Coast (Fig. 5b), although none of these changes passed significance by the FDR procedure (Fig. 5d). While southwestern CONUS had large regions of dramatic change, the lack of spatial coherence lowers our confidence in the ability of our method to detect a regional trend if one did exist.

There were no significant decadal trends at $\alpha = 0.05$ in response time at the NCEI climate regions (Fig. 6). This lack of regional significance is somewhat comparable to previous results. Huntington et al. (2018) found only two out of nine regions (defined through a clustering procedure) with significant annual trends in WCI (P+E) from 1945-2014 at $\alpha = 0.05$.

Decadal response times displayed large increases in the Southwest and West NCEI regions between 1970-2000. While initially disconcerting, this result is perhaps not entirely unexpected given the structure of the lagged correlation relationship between SPI and SSI, including the presence of multiple peaks in correlation and lack of prominence in those peaks (Fig. 7). A potential explanation for the multiple peaks in correlation could lie in the reemergence of soil moisture anomalies from previous seasons. Soil moisture anomalies that arise due to precipitation in one year may be "stored" in deeper layers and reemerge in the subsequent year (Kumar et al., 2019). Soil moisture in the top meter would then be correlated with both recent and earlier precipitation, creating a lagged-correlation relationship with multiple peaks. In the southwestern and western US, the reemergence in the root zone (0-0.4 m) was reported to happen on the order of 6-12 months when looking at JJA soil moisture anomalies using the NCAR Community Land Model (Kumar et al., 2019), aligning reasonably well with the secondary or even tertiary peaks we observed (Fig. 7a-d). As discussed in Sect. 3.4, large shifts in the response time between decades may represent the calculated response time shifting between two local peaks, rather than a shift in timing of one individual peak in correlation. Despite this

https://doi.org/10.5194/egusphere-2026-2895
Preprint. Discussion started: 18 June 2026

explanation, this presence of multiple peaks in correlation and lack of prominence in those peaks raises valid questions about the usefulness of the response time definition of hydrological cycle acceleration in the arid southwest.

4.3 Limitations

The temporal domain of our analysis may obscure or overemphasize certain changes. For example, Huntington et al (2018) found that two out of nine regions showed significant trends in WCI from 1945-2014, but that six out of nine showed significant trends from 1900-2014. Uncertainty can also arise in the decision of how to split the temporal and spatial domain. Our primary analysis (Fig. 5) splits the data into an early and late period, as response time appears to need longer time periods to stabilize. We analyzed at the grid-cell level, treating each model grid cell as an independent hydrological unit. However, comparing between an early and late period and at such a fine spatial resolution may highlight changes specific to those spatial and temporal domains. We attempted to account for spatial and temporal uncertainties by analyzing the decadal trend in response times at the NCEI regional level (Fig. 6). That exposition provided important contextualization to our results, as no region had a significant trend in response.

Additionally, our choice to avoid frozen soils by using only the JJA time series of SSI limits the interpretation of our results to the summer hydrological cycle. Important accelerations or decelerations may be happening at other times in the hydrological cycle, such as earlier and slower snowmelt (Musselman et al., 2017).

Our choices of drought indices, while the product of a reasoned decision to measure the response time between meteorological and soil moisture anomalies, are not the only possible choices. For example, the Standardized Precipitation and Evapotranspiration Index (Vicente-Serrano et al., 2010), or SPEI, has emerged as a popular alternative to the SPI to measure atmospheric/meteorological drought and may produce different response times with SSI. Future work could also apply our definition of hydrological cycle velocity to other anomaly types, such as the response time between meteorological anomalies and streamflow anomalies.

While the RF analysis was crucial to identifying factors associated with the spatial distribution of response time, the results must be interpreted cautiously. Permutation importance scores and partial dependence plots do not establish causality. Rather, they indicate which variables most influence model performance and summarize average model behavior. Despite our clustering technique, several predictors remain strongly correlated (e.g. mean annual precipitation and mean summer precipitation). Although RF predictive skill is generally robust to multicollinearity, correlated predictor variables can share explanatory power, distributing variable importance across correlated variables and complicating the interpretation of individual importance scores.

A key gap that remains is an understanding of potential drivers of the *change* in response time between time periods. Attempts to apply our RF approach to predict temporal changes in response time yielded insufficient predictive skill. This may indicate that important drivers of response time change are missing from our model. Future work incorporating variables such as precipitation intermittency, precipitation extremes and land cover change could open the door to a better understanding of response time changes.

Our application of moving blocks bootstrapping and FDR corrections to test the significance of changes in response times (Fig. 5c-d) follows established best practices. However, these procedures may reduce statistical power: the ability of a statistical test to pick up a significant signal where one exists. The FDR procedure seeks to limit the amount

https://doi.org/10.5194/egusphere-2026-2895
Preprint. Discussion started: 18 June 2026

of Type I errors (incorrectly rejected null hypotheses), thus reducing statistical power. To contextualize this limitation, we present non-FDR-corrected significance results (Fig. 5c). The temporal autocorrelation addressed by the moving blocks bootstrapping may also constrain statistical power. The use of a 90-day block size reduces the early time period to effectively 35 true resample units, i.e., one sample per year, potentially limiting sensitivity. While we consider 90 days to be the appropriate block size, alternative block sizes could result in meaningfully different levels of statistical significance.

A final source of uncertainty in our conclusions is the reliance on the ERA5-Land dataset. Reanalysis products provide a physically consistent and spatially complete framework for assessing hydrological change. Yet, they are inherently uncertain, and different reanalysis products can produce distinct representations of hydrological cycle changes (Vargas Godoy and Markonis, 2023). ERA5-Land does not directly assimilate land surface observations, relying instead on the CHTESSEL land surface model (Muñoz-Sabater et al., 2021). Although ERA5-Land generally compares favorably to available observations (Sect. 2.4), validation is somewhat constrained by the sparse and inconsistent measurement of key variables such as soil moisture. Despite the relatively fine spatial resolution (~0.1°) of ERA5-Land, sub-resolution heterogeneity in soil and vegetation characteristics has the potential to modulate local acceleration. A future evaluation of whether spatial patterns in response time identified here are consistent across multiple data products would be useful to evaluate the robustness of response time as a metric of hydrological acceleration.

5 Conclusions

We introduce a new metric of hydrological cycle velocity based on the response time of JJA SSI-30 to SPI-30. Calculated using ERA5-Land reanalysis data from 1950-2020, response times were longest in southwestern CONUS (on the order of 100-200 days), and shortest in the Great Plains and eastern CONUS (on the order of 10-20 days). Random forest variable importance analysis indicates that mean annual precipitation and evapotranspiration were strongly associated with spatial patterns in response times. Areas with lower flux magnitudes tend to exhibit longer response times, whereas areas with higher flux magnitudes tend to exhibit shorter response times.

Defining hydrological cycle acceleration as the change in response time of JJA SSI-30 to SPI-30, between an early (1951-1985) and late (1986-2020) time period, we showed that a slightly larger proportion of CONUS grid cells experienced a deceleration (48.47 %) than acceleration (39.32 %). Acceleration was most evident in the Great Plains and mid-Atlantic, while deceleration was most evident in the upper Midwest and South, despite none of these passing FDR significance. In the Southwest, substantial spatial variability and large changes in response time complicate the identification of coherent regional trends. At the scale of NCEI climate regions, no significant decadal trends in acceleration or deceleration were detected, reinforcing the finding that observed changes between 1951-1985 and 1986-2020 were not statistically significant.

Importantly, we wish to clarify that the absence of significant changes in response time between the two periods should not be interpreted as definitive evidence that such trends do not exist or will not emerge in the future. Comparable studies have found stronger signals of hydrological cycle change in more recent, or future, time periods (Feng et al., 2017; Wang et al., 2023), potentially due to improved data reliability or increased warming signals.

https://doi.org/10.5194/egusphere-2026-2895
Preprint. Discussion started: 18 June 2026

Future work should further evaluate how shifts reflect broader changes to the hydrological cycle. Extending this framework to later stages of drought propagation—such as the lag between meteorological and streamflow anomalies—could provide insights into different elements of hydrological cycle acceleration. Incorporating additional variables, including precipitation intermittency, extremes, and land cover change may improve understanding of mechanisms underlying shifts in response time. Finally, assessing the robustness of our results across alternative data sources and temporal domains will be critical to understand the transferability of our results.

Overall, while we find some evidence of hydrological acceleration and deceleration across CONUS, we report no statistically significant signal. If significant changes were to be found, they would have practical implications for land and water managers. In the context of drought early warning systems, an accelerating hydrological cycle may reduce the early warning value SPI for agricultural drought, while a decelerating cycle may enhance it. By framing hydrological acceleration in terms of the coupling of hydrological systems, this study offers an important perspective to assessments of hydrological cycle changes over recent decades.

Code and data availability

All data products used in the analysis are publicly available. The precipitation, soil moisture, temperature, PET, evapotranspiration were obtained from ERA5-Land (Muñoz-Sabater et al., 2021), available through the ECMWF (https://doi.org/10.24381/cds.e9c9c792). The repository (Sabin, 2026) containing code for processing the ERA5-Land data into drought indices, calculating acceleration metrics, and building random forest model is available at (https://doi.org/10.5281/zenodo.20277374)

Supplement link

The link to the supplement will be included by Copernicus, if applicable.

Author contributions

Matthew Sabin, Nels Bjarke, and Ben Livneh conceptualized the analysis, and Matthew Sabin conducted the analysis. Matthew Sabin prepared the manuscript with contributions from all co-authors.

Competing interests

The authors declare that they have no conflict of interest.

Disclaimer

Copernicus Publications remains neutral with regard to jurisdictional claims made in the text, published maps, institutional affiliations, or any other geographical representation in this paper. While Copernicus Publications makes

https://doi.org/10.5194/egusphere-2026-2895
Preprint. Discussion started: 18 June 2026

every effort to include appropriate place names, the final responsibility lies with the authors. Views expressed in the text are those of the authors and do not necessarily reflect the views of the publisher.

Acknowledgements

This work utilized the Alpine High-Performance Computing resource at the University of Colorado Boulder. Alpine is jointly funded by the University of Colorado Boulder, the University of Colorado Anschutz, Colorado State University, and the National Science Foundation (award 2201538).
AI tools (ChatGPT and Claude) were used to assist with coding tasks.

Financial support

This research has been supported by the National Oceanic and Atmospheric Administration (Improving drought indices in consideration of nonstationarity (grant no.NA22OAR4320151)).

https://doi.org/10.5194/egusphere-2026-2895
Preprint. Discussion started: 18 June 2026

References

Adler, R. F., Gu, G., Sapiano, M., Wang, J.-J., and Huffman, G. J.: Global Precipitation: Means, Variations and Trends During the Satellite Era (1979–2014), Surv. Geophys., 38, 679–699, https://doi.org/10.1007/s10712-017-9416-4, 2017.

Allen, M. R. and Ingram, W. J.: Constraints on future changes in climate and the hydrologic cycle, Nature, 419, 224–232, https://doi.org/10.1038/nature01092, 2002.

Barker, L. J., Hannaford, J., Chiverton, A., and Svensson, C.: From meteorological to hydrological drought using standardised indicators, Hydrol. Earth Syst. Sci., 20, 2483–2505, https://doi.org/10.5194/hess-20-2483-2016, 2016.

Beck, H. E., Pan, M., Miralles, D. G., Reichle, R. H., Dorigo, W. A., Hahn, S., Sheffield, J., Karthikeyan, L., Balsamo, G., Parinussa, R. M., van Dijk, A. I. J. M., Du, J., Kimball, J. S., Vergopolan, N., and Wood, E. F.: Evaluation of 18 satellite- and model-based soil moisture products using in situ measurements from 826 sensors, Hydrol. Earth Syst. Sci., 25, 17–40, https://doi.org/10.5194/hess-25-17-2021, 2021.

Bell, B., Hersbach, H., Simmons, A., Berrisford, P., Dahlgren, P., Horányi, A., Muñoz-Sabater, J., Nicolas, J., Radu, R., Schepers, D., Soci, C., Villaume, S., Bidlot, J.-R., Haimberger, L., Woollen, J., Buontempo, C., and Thépaut, J.-N.: The ERA5 global reanalysis: Preliminary extension to 1950, Q. J. R. Meteorol. Soc., 147, 4186–4227, https://doi.org/10.1002/qj.4174, 2021.

Benjamini, Y. and Hochberg, Y.: Controlling the False Discovery Rate: A Practical and Powerful Approach to Multiple Testing, J. R. Stat. Soc. Ser. B Methodol., 57, 289–300, https://doi.org/10.1111/j.2517-6161.1995.tb02031.x, 1995.

Bosilovich, M. G., Schubert, S. D., and Walker, G. K.: Global Changes of the Water Cycle Intensity, https://doi.org/10.1175/JCLI3357.1, 2005.

Breiman, L.: Random Forests, Mach. Learn., 45, 5–32, https://doi.org/10.1023/A:1010933404324, 2001.

Brubaker, K. L. and Entekhabi, D.: Asymmetric Recovery from Wet versus Dry Soil Moisture Anomalies, J. Appl. Meteorol. Climatol., 35, 94–109, https://doi.org/10.1175/1520-0450(1996)035%3C0094:ARFWVD%3E2.0.CO;2, 1996.

Budyko, M. I. and Miller, D. H.: Climate and Life, 1974.

Cammalleri, C., McCormick, N., Spinoni, J., and Nielsen-Gammon, J. W.: An Analysis of the Lagged Relationship between Anomalies of Precipitation and Soil Moisture and Its Potential Role in Agricultural Drought Early Warning, https://doi.org/10.1175/JAMC-D-23-0077.1, 2024.

Carrão, H., Russo, S., Sepulcre-Canto, G., and Barbosa, P.: An empirical standardized soil moisture index for agricultural drought assessment from remotely sensed data, Int. J. Appl. Earth Obs. Geoinformation, 48, 74–84, https://doi.org/10.1016/j.jag.2015.06.011, 2016.

Contractor, S., Donat, M. G., and Alexander, L. V.: Changes in Observed Daily Precipitation over Global Land Areas since 1950, https://doi.org/10.1175/JCLI-D-19-0965.1, 2021.

Dai, A.: Increasing drought under global warming in observations and models, Nat. Clim. Change, 3, 52–58, https://doi.org/10.1038/nclimate1633, 2013.

Dai, A.: Historical and Future Changes in Streamflow and Continental Runoff, in: Terrestrial Water Cycle and Climate Change, American Geophysical Union (AGU), 17–37, https://doi.org/10.1002/9781118971772.ch2, 2016.

https://doi.org/10.5194/egusphere-2026-2895
Preprint. Discussion started: 18 June 2026

ECMWF: ERA5-Land: data documentation, 2025.

Efron, B. and Tibshirani, R.: An introduction to the bootstrap / Bradley Efron and Robert J. Tibshirani., Chapman & Hall, 1994.

Feng, H., Zou, B., and Luo, J.: Coverage-dependent amplifiers of vegetation change on global water cycle dynamics, J. Hydrol., 550, 220–229, https://doi.org/10.1016/j.jhydrol.2017.04.056, 2017.

Gevaert, A. I., Veldkamp, T. I. E., and Ward, P. J.: The effect of climate type on timescales of drought propagation in an ensemble of global hydrological models, Hydrol. Earth Syst. Sci., 22, 4649–4665, https://doi.org/10.5194/hess-22-4649-2018, 2018.

Gimeno, L., Eiras-Barca, J., Durán-Quesada, A. M., Dominguez, F., van der Ent, R., Sodemann, H., Sánchez-Murillo, R., Nieto, R., and Kirchner, J. W.: The residence time of water vapour in the atmosphere, Nat. Rev. Earth Environ., 2, 558–569, https://doi.org/10.1038/s43017-021-00181-9, 2021.

Giorgi, F., Im, E.-S., Coppola, E., Diffenbaugh, N. S., Gao, X. J., Mariotti, L., and Shi, Y.: Higher Hydroclimatic Intensity with Global Warming, https://doi.org/10.1175/2011JCLI3979.1, 2011.

Hao, Z. and AghaKouchak, A.: Multivariate Standardized Drought Index: A parametric multi-index model, Adv. Water Resour., 57, 12–18, https://doi.org/10.1016/j.advwatres.2013.03.009, 2013.

Hastie, T., Tibshirani, R., and Friedman, J.: The Elements of Statistical Learning, Springer, 2009.

Hawkes, K., McClaran, M., Brugger, J., Crimmins, M., Howery, L., Ruyle, G., Sprinkle, J., and Tolleson, D.: Guide to Co-Developing Drought Preparation Plans for Livestock Grazing on Southwest National Forests, College of Agriculture and Life Sciences, University of Arizona, 2018.

Hayes, M., Svoboda, M., Wall, N., and Widhalm, M.: The Lincoln Declaration on Drought Indices: Universal Meteorological Drought Index Recommended, Bull. Am. Meteorol. Soc., 92, 485–488, https://doi.org/10.1175/2010BAMS3103.1, 2011.

Held, I. M. and Soden, B. J.: Robust Responses of the Hydrological Cycle to Global Warming, https://doi.org/10.1175/JCLI3990.1, 2006.

Hersbach, H., Bell, B., Berrisford, P., Hirahara, S., Horányi, A., Muñoz-Sabater, J., Nicolas, J., Peubey, C., Radu, R., Schepers, D., Simmons, A., Soci, C., Abdalla, S., Abellan, X., Balsamo, G., Bechtold, P., Biavati, G., Bidlot, J., Bonavita, M., De Chiara, G., Dahlgren, P., Dee, D., Diamantakis, M., Dragani, R., Flemming, J., Forbes, R., Fuentes, M., Geer, A., Haimberger, L., Healy, S., Hogan, R. J., Hólm, E., Janisková, M., Keeley, S., Laloyaux, P., Lopez, P., Lupu, C., Radnoti, G., de Rosnay, P., Rozum, I., Vamborg, F., Villaume, S., and Thépaut, J.-N.: The ERA5 global reanalysis, Q. J. R. Meteorol. Soc., 146, 1999–2049, https://doi.org/10.1002/qj.3803, 2020.

Hobeichi, S., Abramowitz, G., Ukkola, A. M., De Kauwe, M., Pitman, A., Evans, J. P., and Beck, H.: Reconciling historical changes in the hydrological cycle over land, Npj Clim. Atmospheric Sci., 5, 1–9, https://doi.org/10.1038/s41612-022-00240-y, 2022.

Huntington, T. G., Weiskel, P. K., Wolock, D. M., and McCabe, G. J.: A new indicator framework for quantifying the intensity of the terrestrial water cycle, J. Hydrol., 559, 361–372, https://doi.org/10.1016/j.jhydrol.2018.02.048, 2018.

Jeong, M.-S., Park, S.-Y., Kim, Y.-J., Yoon, H.-C., and Lee, J.-H.: Identification of propagation characteristics from meteorological drought to hydrological drought using daily drought indices and lagged correlations analysis, J. Hydrol. Reg. Stud., 55, 101939, https://doi.org/10.1016/j.ejrh.2024.101939, 2024.

Jin, L., Chen, S., Yang, H., and Zhang, C.: Evaluation and Drivers of Four Evapotranspiration Products in the Yellow River Basin, Remote Sens., 16, https://doi.org/10.3390/rs16111829, 2024.

https://doi.org/10.5194/egusphere-2026-2895
Preprint. Discussion started: 18 June 2026

Jung, M., Reichstein, M., Ciais, P., Seneviratne, S. I., Sheffield, J., Goulden, M. L., Bonan, G., Cescatti, A., Chen, J., de Jeu, R., Dolman, A. J., Eugster, W., Gerten, D., Gianelle, D., Gobron, N., Heinke, J., Kimball, J., Law, B. E., Montagnani, L., Mu, Q., Mueller, B., Oleson, K., Papale, D., Richardson, A. D., Roupsard, O., Running, S., Tomelleri, E., Viovy, N., Weber, U., Williams, C., Wood, E., Zaehle, S., and Zhang, K.: Recent decline in the global land evapotranspiration trend due to limited moisture supply, Nature, 467, 951–954, https://doi.org/10.1038/nature09396, 2010.

Kao, A., Jiang, X., Li, L., Trammell, J. H., Zhang, G. J., Su, H., Jiang, J. H., and Yung, Y. L.: A Comparative Study of Atmospheric Moisture Recycling Rate between Observations and Models, https://doi.org/10.1175/JCLI-D-17-0421.1, 2018.

Karl, T. and Koss, W. J.: Regional and national monthly, seasonal, and annual temperature weighted by area, 1895-1983, 1984.

Kumar, S., Newman, M., Wang, Y., and Livneh, B.: Potential Reemergence of Seasonal Soil Moisture Anomalies in North America, J. Clim., 32, 2707–2734, 2019.

Lema, F., Mendoza, P. A., Vásquez, N. A., Mizukami, N., Zambrano-Bigiarini, M., and Vargas, X.: Technical note: What does the Standardized Streamflow Index actually reflect? Insights and implications for hydrological drought analysis, Hydrol. Earth Syst. Sci., 29, https://doi.org/10.5194/hess-29-1981-2025, 2025.

Li, L., Jiang, X., Chahine, M. T., Olsen, E. T., Fetzer, E. J., Chen, L., and Yung, Y. L.: The recycling rate of atmospheric moisture over the past two decades (1988–2009), Environ. Res. Lett., 6, 034018, https://doi.org/10.1088/1748-9326/6/3/034018, 2011.

Liu, C. and Allan, R. P.: Observed and simulated precipitation responses in wet and dry regions 1850–2100, Environ. Res. Lett., 8, 034002, https://doi.org/10.1088/1748-9326/8/3/034002, 2013.

Livneh, B., Bjarke, N. R., Modi, P. A., Furman, A., Ficklin, D., Pflug, J. M., and Karnauskas, K. B.: Can precipitation intermittency predict flooding?, Sci. Total Environ., 945, 173824, https://doi.org/10.1016/j.scitotenv.2024.173824, 2024.

McColl, K. A., Wang, W., Peng, B., Akbar, R., Short Gianotti, D. J., Lu, H., Pan, M., and Entekhabi, D.: Global characterization of surface soil moisture drydowns, Geophys. Res. Lett., 44, 3682–3690, https://doi.org/10.1002/2017GL072819, 2017a.

McColl, K. A., Alemohammad, S. H., Akbar, R., Konings, A. G., Yueh, S., and Entekhabi, D.: The global distribution and dynamics of surface soil moisture | Nature Geoscience, Nat. Geosci., 10, 100–104, https://doi.org/https://doi-org.colorado.idm.oclc.org/10.1038/ngeo2868, 2017b.

McKee, T. B., Doesken, N. J., and Kleist, J.: The relationship of drought frequency and duration to time scales, Proc. 8th Conf. Appl. Climatol., 17, 179–183, 1993.

Mo, K. C.: Drought onset and recovery over the United States, J. Geophys. Res. Atmospheres, 116, https://doi.org/10.1029/2011JD016168, 2011.

Muñoz-Sabater, J., Dutra, E., Agustí-Panareda, A., Albergel, C., Arduini, G., Balsamo, G., Boussetta, S., Choulga, M., Harrigan, S., Hersbach, H., Martens, B., Miralles, D. G., Piles, M., Rodríguez-Fernández, N. J., Zsoter, E., Buontempo, C., and Thépaut, J.-N.: ERA5-Land: a state-of-the-art global reanalysis dataset for land applications, Earth Syst. Sci. Data, 13, 4349–4383, https://doi.org/10.5194/essd-13-4349-2021, 2021.

Musselman, K. N., Clark, M. P., Liu, C., Ikeda, K., and Rasmussen, R.: Slower snowmelt in a warmer world, Nat. Clim. Change, 7, 214–219, https://doi.org/10.1038/nclimate3225, 2017.

https://doi.org/10.5194/egusphere-2026-2895
Preprint. Discussion started: 18 June 2026

Ohmura, A. and Wild, M.: Is the Hydrological Cycle Accelerating?, Science, 298, 1345–1346, https://doi.org/10.1126/science.1078972, 2002.

Pedregosa, F., Pedregosa, F., Varoquaux, G., Varoquaux, G., Org, N., Gramfort, A., Gramfort, A., Michel, V., Michel, V., Fr, L., Thirion, B., Thirion, B., Grisel, O., Grisel, O., Blondel, M., Prettenhofer, P., Prettenhofer, P., Weiss, R., Dubourg, V., Dubourg, V., Vanderplas, J., Passos, A., Tp, A., and Cournapeau, D.: Scikit-learn: Machine Learning in Python, JMLR, 12, 2825–2830, 2011.

Roberts, D. R., Bahn, V., Ciuti, S., Boyce, M. S., Elith, J., Guillera-Arroita, G., Hauenstein, S., Lahoz-Monfort, J. J., Schröder, B., Thuiller, W., Warton, D. I., Wintle, B. A., Hartig, F., and Dormann, C. F.: Cross-validation strategies for data with temporal, spatial, hierarchical, or phylogenetic structure, Ecography, 40, 913–929, https://doi.org/10.1111/ecog.02881, 2017.

Rondinelli, W. J., Hornbuckle, B. K., Patton, J. C., Cosh, M. H., Walker, V. A., Carr, B. D., and Logsdon, S. D.: Different Rates of Soil Drying after Rainfall Are Observed by the SMOS Satellite and the South Fork in situ Soil Moisture Network, J. Hydrometeorol., 16, 889–903, https://doi.org/10.1175/JHM-D-14-0137.1, 2015.

Sabin, M.: Code and outputs for Assessing summertime hydrological cycle acceleration through drought indices., , https://doi.org/10.5281/zenodo.20277374, 2026.

Shellito, P. J., Small, E. E., Colliander, A., Bindlish, R., Cosh, M. H., Berg, A. A., Bosch, D. D., Caldwell, T. G., Goodrich, D. C., McNairn, H., Prueger, J. H., Starks, P. J., van der Velde, R., and Walker, J. P.: SMAP soil moisture drying more rapid than observed in situ following rainfall events, Geophys. Res. Lett., 43, 8068–8075, https://doi.org/10.1002/2016GL069946, 2016.

Svoboda, M., LeComte, D., Hayes, M., Heim, R., Gleason, K., Angel, J., Rippey, B., Tinker, R., Palecki, M., Stooksbury, D., Miskus, D., and Stephens, S.: THE DROUGHT MONITOR, https://doi.org/10.1175/1520-0477-83.8.1181, 2002.

Svoboda, M. D. and Fuchs, B. A.: Handbook of drought indicators and indices, World Meteorological Organization, Geneva, 2016.

Tarek, M., Brissette, F. P., and Arsenault, R.: Evaluation of the ERA5 reanalysis as a potential reference dataset for hydrological modelling over North America, Hydrol. Earth Syst. Sci., 24, 2527–2544, https://doi.org/10.5194/hess-24-2527-2020, 2020.

Trenberth, K.: Changes in precipitation with climate change, Clim. Res., 47, 123–138, https://doi.org/10.3354/cr00953, 2011.

Valavi, R., Elith, J., Lahoz-Monfort, J. J., and Guillera-Arroita, G.: blockCV: an R package for generating spatially or environmentally separated folds for k-fold cross-validation of species distribution models, https://doi.org/10.1101/357798, 28 June 2018.

Van Loon, A. F., Van Huijgevoort, M. H. J., and Van Lanen, H. a. J.: Evaluation of drought propagation in an ensemble mean of large-scale hydrological models, Hydrol. Earth Syst. Sci., 16, 4057–4078, https://doi.org/10.5194/hess-16-4057-2012, 2012.

Vargas Godoy, M. R. and Markonis, Y.: Water cycle changes in reanalyses: a complementary framework, Sci. Rep., 13, 4795, https://doi.org/10.1038/s41598-023-31873-5, 2023.

Vicente-Serrano, S. M., Beguería, S., and López-Moreno, J. I.: A Multiscalar Drought Index Sensitive to Global Warming: The Standardized Precipitation Evapotranspiration Index, https://doi.org/10.1175/2009JCLI2909.1, 2010.

Vicente-Serrano, S. M., Lopez-Moreno, J.-I., Beguería, S., Lorenzo-Lacruz, J., Sanchez-Lorenzo, A., García-Ruiz, J. M., Azorin-Molina, C., Morán-Tejeda, E., Revuelto, J., Trigo, R., Coelho, F., and Espejo, F.: Evidence of increasing

https://doi.org/10.5194/egusphere-2026-2895
Preprint. Discussion started: 18 June 2026

drought severity caused by temperature rise in southern Europe, Environ. Res. Lett., 9, 044001, https://doi.org/10.1088/1748-9326/9/4/044001, 2014.

Vicente-Serrano, S. M., Peña-Angulo, D., Beguería, S., Domínguez-Castro, F., Tomás-Burguera, M., Noguera, I., Gimeno-Sotelo, L., and El Kenawy, A.: Global drought trends and future projections, Philos. Trans. R. Soc. Math. Phys. Eng. Sci., 380, 20210285, https://doi.org/10.1098/rsta.2021.0285, 2022.

Wang, Y., Meili, N., and Fatichi, S.: Evidence and Controls of the Acceleration of the Hydrological Cycle Over Land, Water Resour. Res., 59, e2022WR033970, https://doi.org/10.1029/2022WR033970, 2023.

Wilks, D. S.: "The Stippling Shows Statistically Significant Grid Points": How Research Results are Routinely Overstated and Overinterpreted, and What to Do about It, https://doi.org/10.1175/BAMS-D-15-00267.1, 2016.

Wilks, D. S.: Chapter 5 - Frequentist Statistical Inference, in: Statistical Methods in the Atmospheric Sciences (Fourth Edition), edited by: Wilks, D. S., Elsevier, 143–207, https://doi.org/10.1016/B978-0-12-815823-4.00005-5, 2019.

Williams, A. P., Cook, E. R., Smerdon, J. E., Cook, B. I., Abatzoglou, J. T., Bolles, K., Baek, S. H., Badger, A. M., and Livneh, B.: Large contribution from anthropogenic warming to an emerging North American megadrought, Science, 368, 314–318, https://doi.org/10.1126/science.aaz9600, 2020.

Xiao, M., Udall, B., and Lettenmaier, D. P.: On the Causes of Declining Colorado River Streamflows, Water Resour. Res., 54, 6739–6756, https://doi.org/10.1029/2018WR023153, 2018.

Xu, C., Wang, W., Hu, Y., and Liu, Y.: Evaluation of ERA5, ERA5-Land, GLDAS-2.1, and GLEAM potential evapotranspiration data over mainland China, J. Hydrol. Reg. Stud., 51, 101651, https://doi.org/10.1016/j.ejrh.2023.101651, 2024.

Xu, Y., Wang, L., Ross, K. W., Liu, C., and Berry, K.: Standardized Soil Moisture Index for Drought Monitoring Based on Soil Moisture Active Passive Observations and 36 Years of North American Land Data Assimilation System Data: A Case Study in the Southeast United States, Remote Sens., 10, 301, https://doi.org/10.3390/rs10020301, 2018.

Yeh, P. J.-F. and Wu, C.: Recent Acceleration of the Terrestrial Hydrologic Cycle in the U.S. Midwest, J. Geophys. Res. Atmospheres, 123, 2993–3008, https://doi.org/10.1002/2017JD027706, 2018.

Yuan, X., Wang, Y., Ji, P., Wu, P., Sheffield, J., and Otkin, J. A.: A global transition to flash droughts under climate change, Science, 380, 187–191, https://doi.org/10.1126/science.abn6301, 2023.

Zhang, C. and Ma, Y. (Eds.): Ensemble Machine Learning: Methods and Applications, Springer, New York, NY, https://doi.org/10.1007/978-1-4419-9326-7, 2012.

Zhang, Y., Peña-Arancibia, J. L., McVicar, T. R., Chiew, F. H. S., Vaze, J., Liu, C., Lu, X., Zheng, H., Wang, Y., Liu, Y. Y., Miralles, D. G., and Pan, M.: Multi-decadal trends in global terrestrial evapotranspiration and its components, Sci. Rep., 6, 19124, https://doi.org/10.1038/srep19124, 2016.

Zheng, Y., Coxon, G., Woods, R., Power, D., Rico-Ramirez, M. A., McJannet, D., Rosolem, R., Li, J., and Feng, P.: Evaluation of reanalysis soil moisture products using cosmic ray neutron sensor observations across the globe, Hydrol. Earth Syst. Sci., 28, 1999–2022, https://doi.org/10.5194/hess-28-1999-2024, 2024.

Zhou, Z., Wang, P., Li, L., Fu, Q., Ding, Y., Chen, P., Xue, P., Wang, T., and Shi, H.: Recent development on drought propagation: A comprehensive review, J. Hydrol., 645, 132196, https://doi.org/10.1016/j.jhydrol.2024.132196, 2024.